Immunology & Cell Biology 2025; **103**: 825–843
www.wileyonlinelibrary.com/journal/icb

ORIGINAL ARTICLE

OPEN

Adsorption of antigen to polymeric nanoparticles enhances cytotoxic T-cell responses and anti-tumor immunity by targeting conventional type 1 dendritic cells

Jorge Huete-Carrasco[1], Jingjing Zhu[2,3,4], Benoit J Van den Eynde[2,3,4], Christian Thomas Mayer[5], Tim Sparwasser[6,7], Ross W Ward[1] & Ed C Lavelle[1]

1 Adjuvant Research Group, Trinity Biomedical Sciences Institute, School of Biochemistry and Immunology, Trinity College Dublin, Dublin 2, Ireland
2 Ludwig Institute for Cancer Research, Brussels, Belgium
3 de Duve Institute, Université Catholique de Louvain, Brussels, B-1200, Belgium
4 Walloon Excellence in Life Sciences and Biotechnology, Brussels, Belgium
5 Experimental Immunology Branch, Center for Cancer Research, National Cancer Institute, National Institutes of Health, Bethesda, MD, USA
6 Institute of Medical Microbiology and Hygiene, University Medical Center of the Johannes University Gutenberg, Mainz, Germany
7 Research Center for Immunotherapy, University Medical Centre of the Johannes University Gutenberg, Mainz, Germany

Keywords
Adjuvants, cancer vaccines, conventional type 1 dendritic cells, cytotoxic T cells, immunotherapy, polymeric nanoparticles

Correspondence
Ed C Lavelle, Adjuvant Research Group, School of Biochemistry and Immunology, Trinity Biomedical Sciences Institute, Trinity College Dublin, Dublin 2 D02R590, Ireland.
E-mail: lavellee@tcd.ie

Received 24 April 2025;
Revised 2 and 3 July 2025;
Accepted 3 July 2025

doi: 10.1111/imcb.70049

Immunology & Cell Biology 2025; **103**: 825–843

Abstract

Tumor rejection is primarily mediated by cytotoxic T cells, making them critical targets for therapeutic cancer vaccines. Vaccine adjuvants can modulate innate immunity, influencing adaptive immune responses. For particulate adjuvants, such as polymeric nanoparticles, physicochemical properties—including size, charge, composition and antigen location within the formulation—can shape these responses. Free-soluble antigens typically fail to induce sufficient dendritic cell maturation and cross-presentation needed for robust $CD8^+$ T-cell activation. However, this can be enhanced by delivering antigen with nanoparticles of appropriate size. While adjuvants like oil-in-water emulsions do not require antigen association for vaccine efficacy, the importance of antigen location in the adjuvanticity of polymeric nanoparticles is less clear. We demonstrate that colocalization of antigen and polymeric nanoparticles through antigen adsorption enhances proliferation and activation of antigen-specific $CD8^+$ T cells following intramuscular vaccination. While type 1 conventional dendritic cells (cDC1) can prime $CD8^+$ T cells in other settings, their requirement with polymeric nanoparticles has not been fully addressed. We show that nanoparticle-induced $CD8^+$ T-cell responses rely on cDC1s. The therapeutic efficacy of a polymeric nanoparticle vaccine was significantly enhanced when antigen was adsorbed on nanoparticles, leading to reduced tumor growth and prolonged survival in mice challenged with immunologically hot (MC38) and cold (B16F10) tumors expressing ovalbumin. Furthermore, vaccination with nanoparticle-adsorbed antigen synergized with anti-PD-1 checkpoint blockade, enhancing protection, especially against B16F10-ovalbumin tumors. This work highlights the role of antigen association with polymeric nanoparticles in eliciting $CD8^+$ T-cell responses for the development of effective therapeutic cancer vaccines.

INTRODUCTION

Vaccination is considered one of the major milestones in modern medicine.[1] Prophylactic vaccines can facilitate the control of life-threatening infectious diseases by inducing protection against subsequent exposure to specific pathogens, even reaching eradication, as in the case of smallpox. In addition, therapeutic vaccines have the

potential to control or eliminate chronic infections or tumor cells.[2,3]

Vaccine development has shifted from whole attenuated or inactivated preparations to subunit antigens over recent decades. These vaccines are constituted by purified protein, glycoprotein or polysaccharide antigens. While subunit antigens have advantages in terms of safety, in most cases, these are poorly immunogenic, requiring the addition of adjuvants to increase immunogenicity and enhance vaccine efficacy.[4,5] Adjuvants can serve as immunostimulants in multiple ways, including by acting directly on innate immune cells, particularly dendritic cells (DCs), leading to the activation and modulation of adaptive immunity.[3]

To date, 10 adjuvants have been incorporated into licensed vaccines in humans[6]: Aluminium salts,[7] adjuvant system (AS)04,[8–10] MF59,[11] AS03,[10,12] AS01,[10,13–16] lipid nanoparticles (LNPs),[17,18] Matrix M,[19,20] imidazoquinolin gallamide[21,22], cytosine-phosphate-guanine (CpG) 1018[23,24] and CpG 7909.[25,26] These adjuvants have been especially successful in vaccines against diseases caused by extracellular pathogens or toxins where protection can be mediated by neutralizing antibodies but have proven more limited in the induction of cell-mediated immunity, particularly by cytotoxic $CD8^+$ T cells, which are crucial in the control and protection against cancer.[27] Adjuvant development has historically been an empirical process, which has led to a lack of clarity on how specific adjuvant physicochemical properties (such as size, charge, composition or antigen location in the formulation) affect innate and adaptive immunity. Improved understanding of the mechanism of action of vaccine adjuvants can provide a basis for rational vaccine design and allow tailoring of vaccines for each specific disease and target group.[6]

Conventional dendritic cells (cDCs) play critical roles in the initiation of antigen-specific T-cell responses. While conventional type 2 DCs (cDC2s) preferentially activate antigen-specific $CD4^+$ T cells, they can cross-prime $CD8^+$ T cells in the lungs, mesenteric lymph nodes[28] and tumors.[29] Conventional type 1 DCs (cDC1s) can trigger $CD4^+$ T-cell activation but are specialized in the cross-presentation of exogenous antigens on major histocompatibility complex class I (MHC-I) molecules to activate antigen-specific $CD8^+$ T cells.[6] Thus, cDCs—particularly cDC1s—are key targets for the development of vaccine adjuvants for cancer immunotherapy.

Polymeric particles are an attractive choice as vaccine adjuvants due to their customizable properties, which facilitate rational design to elicit specific types of T-cell responses.[6] We recently demonstrated that size is instructive in the induction of $CD8^+$ T-cell responses by polystyrene (PS) and poly D, L-lactic-co-glycolic acid (PLGA) particles.[30] In the present work, we explored how the location of the antigen influences the efficacy of polymeric nanoparticles as adjuvants for therapeutic cancer vaccines. While mixing antigen with nanoparticles can be effective,[30] free antigen has the potential to promote anergy or regulatory T-cell (Treg) differentiation and potentially antigen-specific tolerance.[31] With some adjuvants such as oil-in-water emulsions, antigen association with the adjuvant is not required for vaccine efficacy, but this is less clear with polymeric nanoparticles. Therefore, we compared the response induced by vaccination with a polymeric nanoparticle formulation where the antigen was adsorbed on the particle surface with a formulation where the antigen was mixed with the particles.

Adsorption of antigen to nanoparticles is principally modulated by electrostatic interactions. Knowing the isoelectric point (pI) of the antigen and adjuvant, it is possible to modulate their charge and consequently, their interaction, by either altering the pH of the buffer in which they are mixed or by changing the pI of the antigen/adjuvant by chemical modifications, such as succinylation or acetylation—to decrease the pI; or aminoamidation—to increase the pI. In addition, the small size of the nanoparticles confers them with higher surface curvature and capacity for protein adsorption.[32,33]

In this work, we demonstrated that intramuscular vaccination (i.m.) with ovalbumin (OVA) adsorbed on 50-nm PS particles led to enhanced expansion and activation of antigen-specific $CD8^+$ T cells by targeting cDC1s and boosting antigen cross-presentation. In a therapeutic setting with mice bearing either hot (MC38) or cold (B16F10) tumors expressing the OVA antigen, we showed that vaccination with OVA adsorbed on 50-nm PS particles induced a significant reduction in tumor growth over time and prolonged the probability of survival to the challenge compared to the mice vaccinated with the nanoparticles mixed with soluble OVA. Moreover, it outperformed the therapeutic effect elicited by the immune checkpoint inhibitor anti-PD-1 monoclonal antibody, and the combination of both therapies showed a synergistic effect in the B16F10-OVA model. Altogether, this work reveals a key role for antigen adsorption in the efficacy of polymeric nanoparticle adjuvants in promoting antigen-specific $CD8^+$ T cells.

RESULTS

Assessment of the colocalization of OVA and 50-nm PS particles upon cellular uptake

To evaluate antigen adsorption to the 50-nm polymeric particles and assess its stability after internalization by

antigen presenting cells (APCs), CD103$^+$ DCs (inducible cDC1s) were stimulated for 20 min with 50-nm PS_{FITC} particles (200 μg mL^{-1}) in the presence of either soluble or adsorbed OVA_{AF647} (5 μg mL^{-1}). The formulation with adsorbed antigen was prepared in HEPES buffer pH 4.5–5.0 (5–8 h incubation at room temperature (RT)), while the formulation with soluble antigen was prepared in PBS pH 7.4 (15–30 min incubation at RT) (Supplementary figure 1). This setup also allowed a comparison of antigen internalization efficiency between the two conditions.

Results show that CD103$^+$ DCs stimulated with the polymeric formulation prepared in HEPES buffer internalized higher amounts of antigen (red signal) compared to the cells stimulated with 50-nm PS particles mixed with OVA in PBS (Figure 1a, b). This finding is supported by a 41.9-fold increase in the OVA_{AF647} mean fluorescence intensity (MFI) (Figure 1c).

Additionally, 47% of the CD103$^+$ DC population stimulated with the polymeric formulation prepared in HEPES buffer were double positive for both OVA_{AF647} and PS_{FITC}, indicating internalization of both antigen and particle, while only 4.3% of cells treated with 50-nm PS particles with soluble antigen in PBS were double positive (Figure 2).

ImageStream analysis (Figure 1a, b) further confirmed enhanced co-localization of antigen and nanoparticle in the cells stimulated with 50-nm polymeric formulation prepared in HEPES buffer, visible as an orange/yellow signal, demonstrating successful antigen adsorption and its stability upon cellular uptake. These observations are further supported by MFI analysis (Figure 2). While OVA_{AF647} MFI increased 2.7-fold compared to the formulation with mixed OVA prepared in PBS as a consequence of antigen adsorption to the nanoparticle surface, the 50-nm PS_{FITC} particle MFI decreased 2.9-fold, suggesting surface masking of the nanoparticle fluorescence by the adsorbed antigen.

Overall, these results demonstrate that the OVA antigen effectively adsorbs to 50-nm PS particles under HEPES buffer conditions and remains stably associated after internalization by CD103$^+$ DCs.

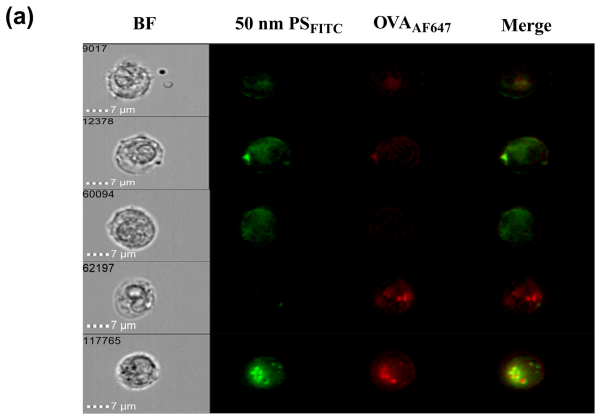

(c)

	50 nm PS with soluble OVA	50 nm PS with adsorbed OVA
MFI OVA_{AF647}	2 715.6	113 755.4

Figure 1. Assessment of the colocalization of OVA and 50-nm PS particles upon cellular uptake. CD103$^+$ DCs were treated with 50-nm PS_{FITC} particles (200 μg mL^{-1}) with either **(a)** soluble or **(b)** adsorbed OVA_{AF647} (5 μg mL^{-1}) for 20 min. Then, cells were fixed and the colocalization of OVA_{AF647} and 50-nm PS_{FITC} particles inside the cells was studied by flow cytometry (4 laser Amnis ImageStream cytometer). Five different cells are shown for each of the treatment groups. Green represents the signal produced by 50-nm PS_{FITC} particles, and red shows the signal provided by OVA_{AF647}. The merged image shows the colocalization of antigen and nanoparticles inside the cells in orange/yellow. **(c)** MFI values of OVA_{AF647} representative of the amount of antigen taken up by CD103$^+$ DCs for each of the treatment groups. Data shown are from one independent experiment.

Adsorption of antigen to 50-nm PS particles significantly enhanced CD8$^+$ T-cell proliferation by conventional type 1 DCs *in vitro*

cDC1s are specialized at cross-presenting exogenous antigens to CD8$^+$ T cells on MHC-I molecules. Experiments were carried out to address whether the cDC1 population could be targeted by 50-nm polymeric particles with OVA and to investigate the role of the antigen adsorption to the nanoparticle surface in the induction of antigen cross-presentation and activation of antigen-specific CD8$^+$ T cells.

CD103$^+$ DCs derived from female C57BL/6J mouse bone marrow (BM) precursors (inducible cDC1s) were stimulated with OVA (10 μg mL^{-1}) either alone or in combination with 50-nm PS particles (400 μg mL^{-1}) for 6 h. Thereafter, cDC1s were cocultured for 72 h with

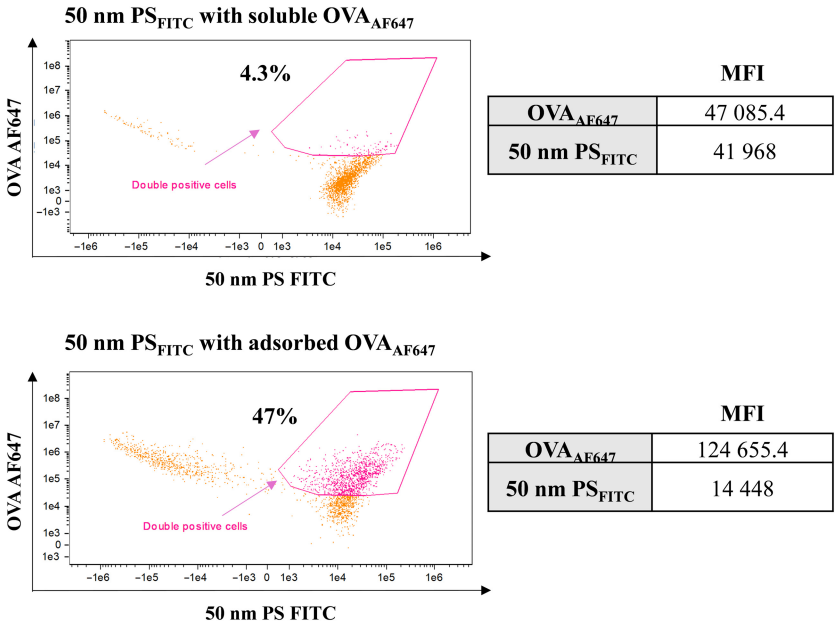

Figure 2. Assessment of the colocalization of OVA and 50-nm PS particles upon cellular uptake. CD103+ DCs were treated with 50-nm PS$_{FITC}$ particles (200 μg mL^{-1}) with either soluble or adsorbed OVA$_{AF647}$ (5 μg mL^{-1}) for 20 min. Then, cells were fixed and the colocalization of OVA$_{AF647}$ and 50-nm PS$_{FITC}$ particles inside the cells was studied by flow cytometry (4 laser Amnis ImageStream cytometer). Dot plots show the percentage of double-positive cells that internalized 50-nm PS$_{FITC}$ particles and OVA$_{AF647}$ as well as the MFI values for antigen and nanoparticles.

CD8+ T cells isolated from OT-I mice, which present a transgenic T-cell receptor recognizing ovalbumin peptide residues 257–264 (OVA$_{257-264}$) in the context of H2K^b MHC-I. These CD8+ T cells were previously stained with carboxyfluorescein succinimidyl ester (CFSE) to assess their proliferation upon crosspresentation of the antigen by CD103+ DCs. CFSE covalently binds to intracellular proteins, and the reduced MFI reflects increased cell proliferation. Indeed, this effect was observed in the cocultures with CD103+ DCs stimulated with 50-nm PS particles, where the formulation with adsorbed OVA (90–95% of antigen adsorbed on the nanoparticle's surface, Supplementary figure 1) significantly enhanced the proliferation of OT-I CD8+ T cells compared with the response elicited by the antigen alone (18.1-fold increase of total number of proliferating CD8+ T cells) (Figure 3). However, this response was less marked in the cocultures with CD103+ DCs stimulated with 50-nm PS particles with soluble OVA (4.1-fold increase of total number of proliferating CD8+ T cells compared with stimulation with OVA alone) (Figure 3).

Therefore, these results show the potential of adsorbing antigen to 50-nm polymeric particles to trigger cDC1s, induce antigen cross-presentation and enhance antigen-specific CD8+ T cell responses.

Vaccination with antigen adsorbed on 50-nm PS particles induces antigen-specific CD8+ T cell responses

Since 50-nm PS particles with adsorbed OVA significantly enhanced DC-induced CD8+ T cell proliferation *in vitro*, the potential of i.m. vaccination with this formulation to induce this type of response was investigated. C57BL/6J mice were immunized by i.m. injection in the hind limbs on days 0 (prime) and 14 (boost) with 5 μg of OVA alone or in combination with 50-nm PS particles (200 μg per mouse), with 90–95% of antigen adsorbed on the nanoparticle surface (Supplementary figure 1).

Activated OVA-specific splenic CD8+ T cells (CD44^{hi}, Tmer+) were determined 2 weeks after booster vaccination by flow cytometry using H-2K^b OVA$_{257-264}$ SIINFEKL epitope tetramers. Vaccination with 50-nm PS particles with adsorbed antigen significantly enhanced induction of antigen-specific CD8+ T cells compared to vaccination with OVA alone (3.6-fold increase in percentage over total CD8+ T cells and 4.9-fold increase in total number in spleen) (Figure 4a, c, d).

IFN-γ produced by activated lymphocytes can enhance cross-presentation by conventional type 1 DCs[34] and activation of CD8+ T cells with sustained cytotoxicity within the tumor microenvironment via IL-12 production.[35] Therefore, we analyzed IFN-γ production by splenic CD8+ T cells by intracellular staining of

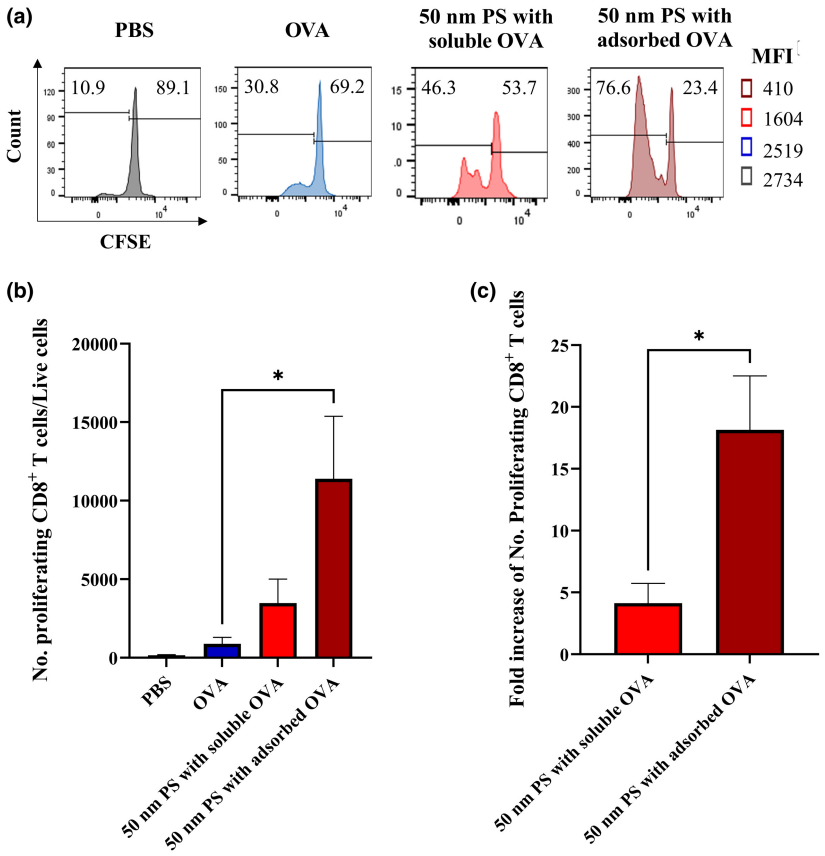

Figure 3. Antigen adsorption to 50-nm PS particles significantly enhances CD8$^+$ T-cell proliferation by conventional type 1 DCs *in vitro*. CD103$^+$ DCs were stimulated with OVA (10 μg mL^{-1}) either alone or in combination with 50-nm PS particles (400 μg mL^{-1}) for 6 h and then cocultured with CFSE-stained OT-I CD8$^+$ T cells for 72 h. **(a)** Representative histograms with the percentage of proliferating and nonproliferating OT-I CD8$^+$ T cells determined by a reduction in CFSE intensity. This is also indicated by the MFI values under the different stimulations. **(b)** A Bar graph showing the mean with SEM of the total number of proliferating OT-I CD8$^+$ T cells over the total live cells with the different stimulations. One-way ANOVA with Tukey's correction for multiple comparisons was applied for the statistical analysis. **(c)** A bar graph representing the mean with SEM of the fold increase of the total number of proliferating OT-I CD8$^+$ T cells obtained after stimulation with each of the PS formulations compared with the stimulation with antigen alone. An unpaired two-tailed *t*-test was applied for the statistical analysis. Data are representative of six independent experiments ($n = 6$), each with one technical replicate. Statistical significance was set at $P \leq 0.05$. *P*-values are represented as $^*P < 0.05$.

restimulated splenocytes. Vaccination with 50-nm PS particles with adsorbed OVA resulted in a significantly higher response compared with mice receiving the antigen alone (3.6-fold increase in percentage of IFN-γ$^+$ CD8$^+$ T cells over total activated CD8$^+$ T cells and 2.1-fold increase in total number of activated IFN-γ$^+$ CD8$^+$ T cells in spleen) (Figure 4b, e, f).

Therefore, these results confirmed that the previously described increase in antigen-specific CD8$^+$ T-cell activation mediated by CD103$^+$ DCs stimulated with the 50-nm PS formulation with adsorbed antigen *in vitro* correlates with the outcomes observed upon vaccination with the same formulation. In addition, 50-nm PS particles with adsorbed antigen elicited the production of antigen-specific IFN-γ by these CD8$^+$ T cells in vaccinated mice.

Induction of CD8$^+$ T-cell responses by vaccination with OVA adsorbed on 50-nm PS particles requires conventional type 1 DCs

cDC1s can trigger the activation of CD4$^+$ T cells, but they are specialized at crosspresenting exogenous antigens to activate CD8$^+$ T cells. However, cDC2s, which excel at activating CD4$^+$ T cells, have also been described to be capable of cross-priming CD8$^+$ T cells in the lungs, mesenteric lymph nodes[28] and in tumors.[29] Therefore, it was important to address whether cDC1s were required

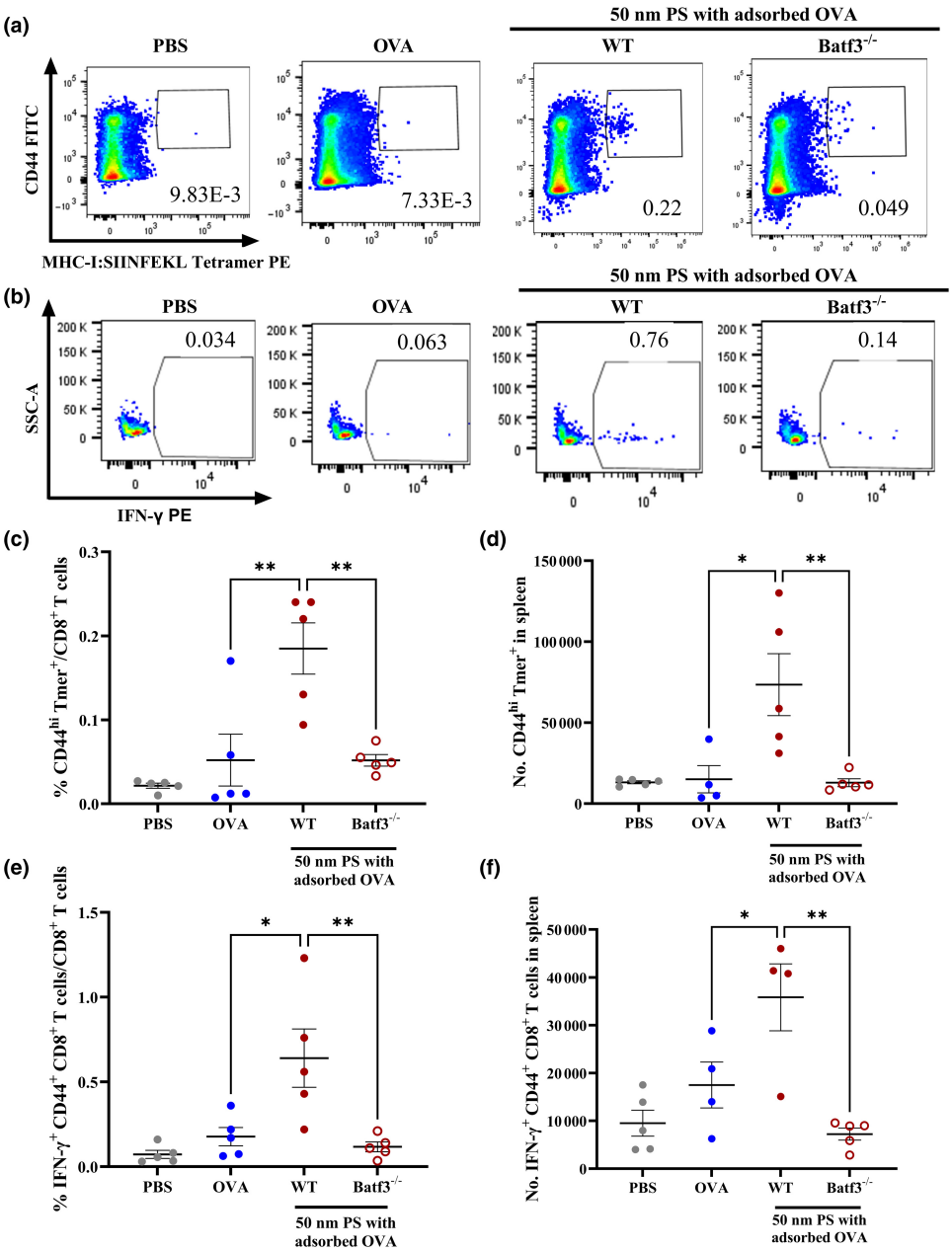

Figure 4. Induction of CD8$^+$ T-cell responses by vaccination with OVA adsorbed on 50-nm PS particles requires conventional type 1 DCs. **(a)** Representative dot plots from WT and Batf3$^{-/-}$ mice immunized with either 5 μg OVA alone or adsorbed on 50-nm PS particles (200 μg per mouse) (n = 5 per group), indicating the percentage of activated CD8$^+$ T cells specific to H-2K^b OVA$_{257-264}$ SIINFEKL epitope (CD44^{hi} Tmer$^+$ CD8$^+$ T cells). This was determined by flow cytometry staining with tetramers 14 days after i.m. booster vaccination. **(b)** A representative dot plot from each of the groups of mice indicating the percentage of IFN-γ$^+$ activated (CD44$^+$) CD8$^+$ T cells after re-stimulation of splenocytes with OVA antigen (200 μg mL^{-1}) and OVA$_{257-264}$ SIINFEKL peptide (1 μg mL^{-1}) for 2 h and a further 12 h in the presence of Golgi Plug (containing Brefeldin A). This was determined by flow cytometry 14 days after i.m. booster vaccination. **(c)** Scatter plots with individual values (n = 5 per group) and mean with SEM of the percentage of activated CD8$^+$ T cells specific to H-2K^b OVA$_{257-264}$ SIINFEKL epitope (CD44^{hi} Tmer$^+$ CD8$^+$ T cells) in each group over the total number of CD8$^+$ T cells, as well as **(d)** the total number of activated antigen-specific CD8$^+$ T cells in spleen (n = 5- PBS and 50-nm PS with adsorbed OVA; n = 4- OVA). **(e)** Scatter plots with individual values (n = 5 per group) and mean with SEM of the percentage of IFN-γ$^+$ CD8$^+$ T cells in each group over the total number of activated (CD44$^+$) CD8$^+$ T cells, as well as **(f)** the total number of activated (CD44$^+$) IFN-γ$^+$ CD8$^+$ T cells in spleen (n = 5- PBS; n = 4- OVA and 50-nm PS with adsorbed OVA). One-way ANOVA with Tukey's correction for multiple comparisons was applied for the statistical analysis. Statistical significance was set at $P \leq 0.05$. P-values are represented as *$P < 0.05$, **$P < 0.005$. Data shown are from one independent experiment with the number of biological replicates indicated above.

for the nanoparticle vaccine-driven CD8$^+$ T cell response described *in vivo*, as this has not been investigated before. C57BL/6J WT and Batf3 deficient mice were vaccinated by i.m. injection with 5 μg of OVA alone or adsorbed on 50-nm PS particles (200 μg per mouse) on day 0 (prime) and 14 (boost). Since Batf3 is a transcription factor required for the differentiation of progenitor cells in BM into cDC1s, Batf3 deficient mice lack this cellular population.[36]

Activated OVA-specific splenic CD8$^+$ T cells (CD44^{hi}, Tmer$^+$) were determined 2 weeks after booster vaccination by flow cytometry using H-2K^b OVA$_{257\text{-}264}$ SIINFEKL epitope tetramers. While vaccination of WT mice with antigen adsorbed on nanoparticles induced a robust antigen-specific CD8$^+$ T cell response (Figure 4a, c, d) and IFN-γ$^+$ CD8$^+$ T cell population (Figure 4b, e, f), this was abrogated in vaccinated Batf3$^{-/-}$ mice (Figure 4).

Thus, these results indicate that the CD8$^+$ T-cell immunity mediated by vaccination with 50-nm PS particles with adsorbed OVA requires cDC1s.

Vaccination with antigen adsorbed on 50-nm PS particles enhanced protection in a therapeutic setting against hot and cold tumors

As previously described, vaccination with antigen adsorbed on polymeric nanoparticles significantly enhanced antigen-specific cytotoxic T cells and IFN-γ responses. Munoz-Wolf *et al.*[30] demonstrated that vaccination with antigen and 50-nm polymeric particles induced CD8$^+$ T cell-dependent anti-tumor protection in a murine melanoma model. Therefore, to determine whether the CD8$^+$ T cells induced by antigen adsorbed on 50-nm PS particles are functionally active in a cancer therapeutic setting and to evaluate the role of the antigen adsorption to nanoparticles, two studies were performed: one against a hot tumor—a murine model of colon adenocarcinoma expressing the OVA protein (MC38-OVA); and another against a cold tumor—a murine model of melanoma expressing the OVA protein (B16F10-OVA). The expression of OVA by the latter makes this tumor model more immunogenic than the parenteral B16F10; nevertheless, its immunogenicity depends on the activation and infiltration of functional antigen-specific T cells, which can be modulated by vaccination.[37] Mice-bearing tumors of 10–20 mm^3 in size were vaccinated by i.m. injection twice, 1 week apart (so that we could administer the two doses of the vaccine before the tumor reached the humane endpoint of 15 mm^3), with PBS, OVA alone (10 μg) or OVA in combination with 50-nm PS particles (400 μg) either adsorbed on the nanoparticle surface or mixed (Figure 5a).

Vaccination with OVA adsorbed on or mixed with 50-nm particles significantly reduced tumor growth over time in mice challenged with MC38-OVA tumor cells compared with the mice receiving OVA alone. Vaccination with the nanoparticle formulation with adsorbed OVA resulted in significantly decreased tumor growth over time compared with the nanoparticle formulation with soluble antigen (Figure 5b). Furthermore, vaccination of mice with OVA adsorbed on but not mixed with 50-nm PS particles significantly increased the probability of survival of mice bearing MC38-OVA tumors (83.3%) compared with the mice receiving the antigen alone (16.7%) (Figure 5c).

In the case of the mice challenged with B16F10-OVA tumor cells, the mice vaccinated with antigen adsorbed on nanoparticles exhibited significantly reduced tumor growth over time compared with the mice receiving either OVA alone or 50-nm PS particles with antigen in solution (Figure 5d). Despite this, there were no significant differences in the probability of survival to B16F10-OVA tumors between treatments (Figure 5e).

Spider plots of individual tumor growth for each of the treatment groups are shown in Supplementary figure 2.

These results demonstrate the importance of antigen adsorption to polymeric nanoparticles to achieve antitumor protection.

Vaccination with antigen adsorbed on 50-nm PS particles synergizes with anti-PD-1 to delay tumor progression

Blocking of coinhibitory or checkpoint molecules by monoclonal antibodies can potentiate and restore antitumor immunity clinically in multiple cancer types, such as (1) CTLA-4 (cytotoxic T lymphocyte associated protein 4)—Ipilimumab (Yervoy) in advanced melanoma and renal cell cancer and (2) PD-1 (programmed cell death protein 1)—Nivolumab (Opdivo) and Pembrolizumab (Keytruda) in melanoma skin cancer, Hodgkin lymphoma and nonsmall-cell lung cancer (NSCLC). Nivolumab is also a treatment for some kidney cancers and head and neck cancers, and Pembrolizumab is used for cancers of the urinary tract; (3) PDL-1 (programmed cell death ligand 1)-Atezolizumab in lung, liver, breast and urothelial cancers, Avelumab in Merkel cell carcinoma and urothelial cancers and Durvalumab in NSCLC.[38,39] However, the number of responders to these therapies remains low.[40] To overcome this challenge, combination approaches have been proposed and demonstrated to correlate with improved response rates.[41]

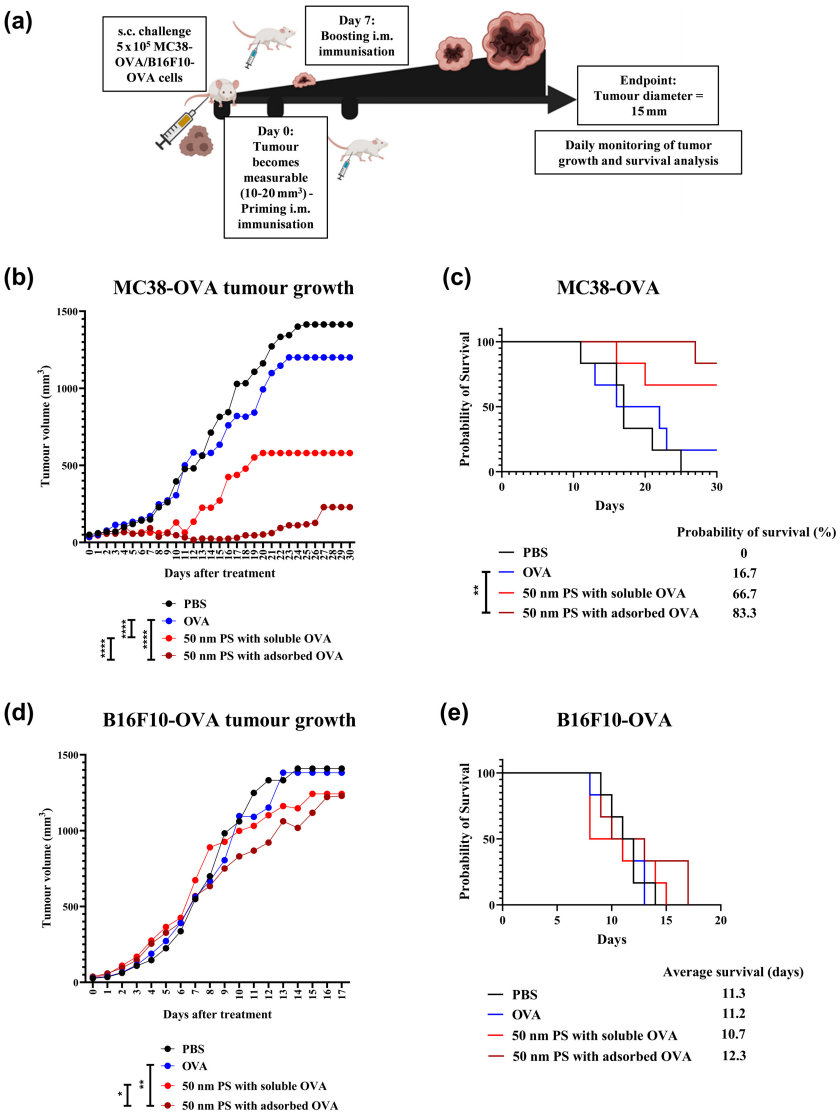

Figure 5. Therapeutic vaccination with antigen adsorbed on 50-nm PS particles enhances protection against MC38-OVA and B16F10-OVA tumor progression. **(a)** 5 × 10^5 MC38-OVA or B16F10-OVA cells were administered by s.c. injection in the lateral flank of C57BL/6J mice. Once tumors reached 10–20 mm^3 (day 0) and 1 week after (day 7), mice were vaccinated i.m. with OVA alone (10 μg) or OVA adsorbed on or mixed with 50-nm PS particles (400 μg). Tumor growth was monitored daily until a humane endpoint of ≥ 15 mm in diameter was reached. **(b, d)** Graphs show the mean MC38-OVA and B16F10-OVA tumor growth of $n = 6$ mice over time for each of the treatments. Statistical differences were determined by two-way ANOVA with Tukey's correction for multiple comparisons. **(c, e)** Graphs show the probability of survival to MC38-OVA and B16F10-OVA tumors ($n = 6$ per group) by treatment groups over 30 and 17 days, respectively. Statistical differences were determined by a simple survival analysis (Kaplan–Meier) with the log-rank (Mantel-Cox) test. Statistical significance was set at $P \leq 0.05$. *$P < 0.05$, **$P < 0.005$, **** $P < 0.0001$. Data shown are from one independent experiment with six biological replicates per group ($n = 6$).

To compare the therapeutic effect achieved by vaccination with 50-nm PS particles with adsorbed antigen with the clinically used anti-PD-1 monotherapy and to assess the synergy between both therapies, C57BL/6J mice bearing either MC38-OVA or B16F10-OVA tumors were vaccinated by i.m. injection twice, 1 week apart, with either PBS or OVA (10 μg) adsorbed on 50-nm PS particles (400 μg). At days 5, 10 and 15 after the first immunization, anti-PD-1 immune checkpoint blockade (200 μg) was administered to the corresponding mice by intraperitoneal (i.p.) injection (Figure 6a).

Mice vaccinated with antigen adsorbed on 50-nm PS particles exhibited significantly reduced tumor growth

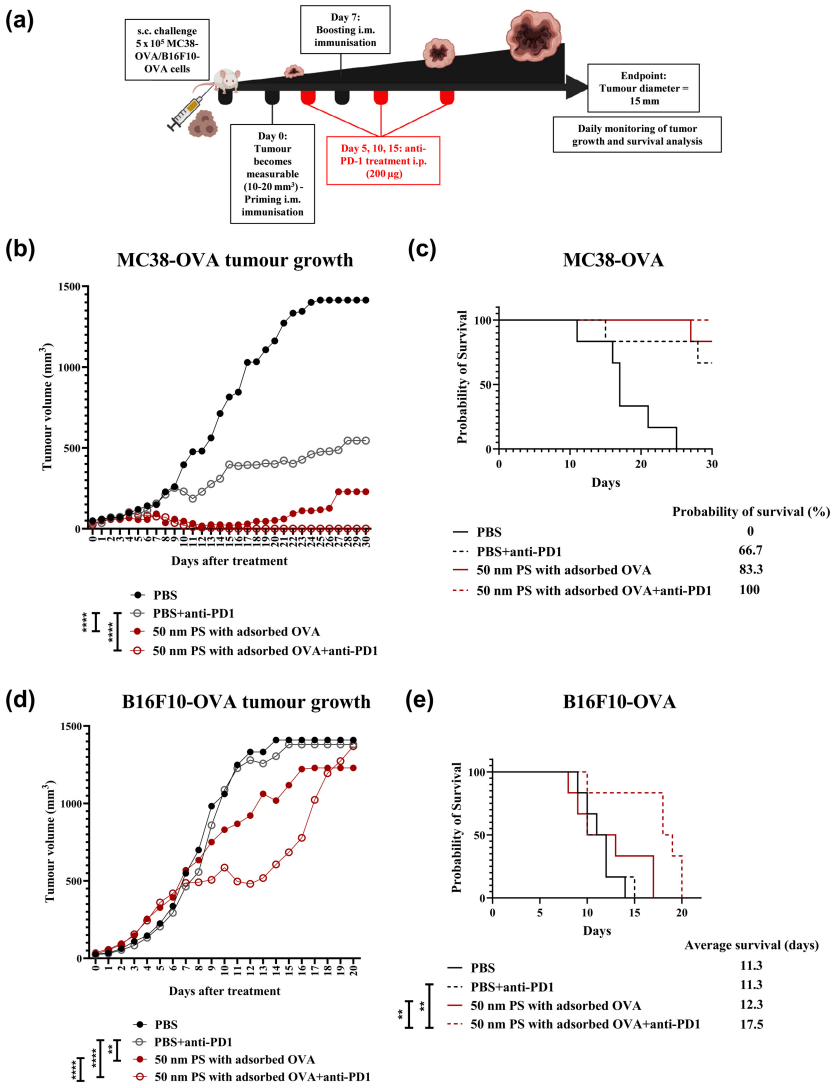

Figure 6. Vaccination with antigen adsorbed on 50-nm PS particles synergizes with anti-PD-1 to delay tumor progression. **(a)** 5 × 10^5 MC38-OVA or B16F10-OVA cells were administered by s.c. injection in the lateral flank of C57BL/6J mice. Once tumors reached 10–20 mm^3 (day 0) and 1 week after (day 7), mice were vaccinated i.m. with either PBS or OVA adsorbed on 50-nm PS particles. At day 5, 10 and 15 after the first immunization, anti-PD-1 immune checkpoint blockade was administered i.p. to the corresponding mice. Tumor growth was monitored daily until a humane endpoint of ≥ 15 mm in diameter was reached. **(b, d)** Graphs show the mean MC38-OVA and B16F10-OVA tumor growth of $n = 6$ mice over time, for each of the treatments. Statistical differences were determined by two-way ANOVA with Tukey's correction for multiple comparisons. **(c, e)** Graphs show the probability of survival to MC38-OVA and B16F10-OVA ($n = 6$ per group) over 30 and 20 days, respectively. Statistical differences were determined by a simple survival analysis (Kaplan–Meier) with the log-rank (Mantel-Cox) test. Statistical significance was set at $P \leq 0.05$. $^{**}P < 0.005$. $^{****}P < 0.0001$. Data shown are from one independent experiment with six biological replicates per group ($n = 6$).

over time compared with mice receiving anti-PD-1 monotherapy in both tumor models (Figure 6b, d). The combination of 50-nm PS particles with adsorbed OVA and anti-PD-1 monoclonal antibody did not result in a therapeutic benefit in MC38-OVA tumors compared with the monotherapy with the nanoparticle formulation alone (Figure 6b, c). However, a clear benefit of combining the nanoparticle-based vaccine with anti-PD-1 was seen in the case of mice-bearing B16F10-OVA tumors, as tumor growth was reduced over time (Figure 6d) and the probability of survival increased (17.5 days) compared with the groups receiving either of the monotherapies alone (anti-PD-1: 11.3 days; 50-nm PS with adsorbed OVA: 12.3 days) (Figure 6e). Spider plots of individual tumor growth for each of the treatment groups are shown in Supplementary figure 3.

These results highlight the need for combination therapies to enhance the activation and infiltration of cytotoxic T cells into the tumor and improve their effector function by PD-1 signaling blockade.

DISCUSSION

Cancer vaccines must trigger protective antigen-specific cell-mediated immunity, including cytotoxic $CD8^+$ T cells and IFN-γ production, so identifying vaccine adjuvants that promote such responses is a priority. It is crucial to understand how specific physicochemical properties of adjuvants modulate vaccine-induced adaptive immune responses to allow tailoring of adjuvants and vaccines for specific objectives.[6] While physical association with the antigen is not essential for the efficacy of some adjuvants such as oil-in-water emulsions, this is less clear with polymeric nanoparticles. We demonstrate that antigen association with polymer nanoparticles enhances vaccine efficacy in promoting protective $CD8^+$ T-cell responses and that cDC1 cells are the key mediators of these responses.

cDCs play critical roles in the initiation of antigen-specific T-cell responses. While cDC2s preferentially activate antigen-specific $CD4^+$ T cells, these cells were recently shown to cross-prime $CD8^+$ T cells in the lungs, mesenteric lymph nodes[28] and tumors.[29] cDC1s can trigger $CD4^+$ T cell activation and are specialized in the cross-presentation of exogenous antigens to activate antigen-specific $CD8^+$ T cells.[6] Therefore, one leading strategy in developing adjuvants to enhance cell-mediated immunity lies in targeting cDCs—specially cDC1s[42]. This can be achieved either by using monoclonal antibodies directed to cell surface molecules—for example, cDC1s can be targeted through CLEC9A antibody presentation on the surface of nanoparticles[43]; or through rational design of the physicochemical properties of vaccine adjuvants to control their distribution to specific tissues.[6]

In this vein, polymeric nanoparticles are an attractive class of vaccine adjuvant due to their stability, biocompatibility and customisable properties, which facilitate rational design to elicit distinct immune responses.[44] In addition, polymeric nanoparticles have been shown to favor internalization by APCs and trafficking to lymph nodes.[3,45] Recently, a polymeric nanoparticle-based vaccine targeting the Stimulator of interferon genes (STING) - Interferon regulatory factor 3 (IRF3) pathway in cDC1s showed enhanced trafficking to tumor-draining lymph nodes, upregulation of costimulatory molecules, antigen cross-presentation, chemokine production, and consequently, a long-lasting $CD8^+$ T-cell-mediated antitumor response in hot and cold tumors.[46]

T-cell-mediated immunity has been shown to be altered depending on the location of the antigen in vaccine formulations. Antigen presentation alone is not sufficient for the induction of effector T cells; as in the absence of adequate costimulation, this can lead to anergy. Therefore, colocalization of adjuvant and antigen can be beneficial.[47] An example of this is the enhanced T helper (Th)1/Th17 response reported by Wørzner *et al.*[31] by adsorbing succinylated lysozyme antigen to the cationic liposomal adjuvant CAF01, by electrostatic interactions.

The high surface area presented by polymeric nanoparticles facilitates the adsorption of vaccine antigens to their surface, creating a pathogen-mimetic structure that can enhance immune responses such as cytotoxic $CD8^+$ T cells.[33,48] This has been associated with a reductive microenvironment upon particle internalization and retention in stable early endosomes, which consequently leads to endosomal rupture, antigen release to the cytosol, cross-presentation and $CD8^+$ T-cell activation.[1,5] Stano *et al.*[5] described a poly(propylene sulfide) and poly(ethylene glycol) nanocarrier with OVA antigen adsorbed on the surface by disulfide bonds that induced stronger antigen-specific $CD8^+$ T cells upon subcutaneous (s.c.) administration in mice compared to the nanoparticles (polymersomes) with encapsulated antigen, which shifted the response toward $CD4^+$ T-cell activation. Furthermore, Nembrini *et al.*[49] demonstrated that the enhanced cytotoxic T-cell response observed upon pulmonary administration of pluronic-stabilized polypropylene sulfide nanoparticles with disulfide bond-conjugated OVA in mice required reduction of these bonds within endosomes upon DC internalization, leading to antigen release into the cytosol followed by antigen cross-presentation.

Munoz-Wolf *et al.*[30] identified a critical role for reactive oxygen species (ROS) and components of the noncanonical inflammasome—caspase 11 and gasdermin D (GSDMD), in the mediation of $CD8^+$ T-cell responses following i.m. vaccination of mice with OVA and 50-nm polymeric particles. In the latter work, the antigen was mixed with the particles, so in the current study, we investigated whether the efficacy of polymer nanoparticles would be further enhanced by adsorbing the antigen to the particles or if simple mixing was sufficient to promote potent cytotoxic T-cell responses and antitumor immunity. We demonstrate that antigen adsorption to 50-nm polymeric particles led to enhanced expansion and activation of antigen-specific $CD8^+$ T cells upon coculture of stimulated $CD103^+$ DCs (inducible cDC1s) with OVA-specific OT-I $CD8^+$ T cells, as well as after i.m. vaccination of WT mice with 50-nm PS particles with adsorbed OVA. Furthermore, by studying the

immune response in vaccinated Batf3 deficient mice (lacking cDC1s[36]), we demonstrated that cDC1s are essential in the induction of CD8$^+$ T-cell responses by 50-nm polymeric particles with adsorbed antigen, which drive a preferential IFN-γ production from CD8$^+$ T cells rather than CD4$^+$ Th1 cells.

We assessed the effector function of the CD8$^+$ T cells driven by vaccination with the polymeric nanoparticle formulation with adsorbed OVA in a therapeutic cancer setting. Two models of murine tumors were used in this study, both expressing the OVA antigen: a colorectal adenocarcinoma (MC38-OVA) and a melanoma cell line (B16F10-OVA). In 2009, Camus *et al.*[50] introduced the classification of tumors based on the equilibrium of anti-tumor immunity and tumor evasion, characterizing their immune features as hot, variable, or cold. MC38 is a hot tumor, characterized by a high infiltration of tumor infiltrating lymphocytes, a preexisting antitumor immune response, overexpression of PDL-1 and therefore, a high rate of response to immunotherapy, especially to immune checkpoint inhibitors (ICI) such as anti-PD-1 monoclonal antibodies[51]; whereas B16F10 is a cold tumor,[52] with poor infiltration of immune cells and limited response to ICI immunotherapy.

Vaccination of mice bearing either MC38-OVA murine colorectal carcinoma cells or B16F10-OVA murine melanoma cells with OVA adsorbed on 50-nm PS particles significantly reduced the tumor growth over time compared with mice receiving either the antigen alone or 50-nm PS with soluble OVA. In addition, the probability of survival of mice to MC38-OVA challenge was also significantly enhanced with the polymeric formulation with adsorbed OVA. This highlights the importance of adsorbing antigen to polymeric nanoparticles to improve the therapeutic effect of cancer vaccines. In the B16F10-OVA model, the significant reduction in tumor growth was not sufficient to enhance the probability of survival of the challenged mice, most likely due to a limited infiltration and effector function of the CD8$^+$ T cells induced upon vaccination with 50-nm PS particles with adsorbed OVA because of a highly immunosuppressive microenvironment present in the tumor.

Monotherapy using ICI, such as PD-1 monoclonal antibody, has shown impressive results in treating multiple types of cancers, including NSCLC and melanoma.[53] PD-1 is a coinhibitory receptor that regulates the proliferation and effector function of tumor-specific T cells by binding with PD-L1 or PD-L2. Despite this, the percentage of responders to ICI monotherapy is still quite low, especially for cold and variable tumors (tumors in a transitional stage in between hot and cold) such as prostate or pancreatic cancers, requiring the combination with therapeutic vaccines.[54–56] The latter would bring antigen-specific cytotoxic T cells to the tumor microenvironment. These cells would upregulate immune checkpoint molecules such as PD-1,[57] but the anti-PD-1 ICI therapy would prevent activated T cells from becoming senescent in the tumor microenvironment, keeping their cytotoxic activity and cytokine production stable for longer and effectively controlling tumor growth.[58]

To determine whether the combination of our therapeutic vaccine with anti-PD-1 monoclonal antibody could enhance the activation of the infiltrated immune cells and generate efficient antitumor immunity, we treated challenged mice with either anti-PD-1 monoclonal antibody, antigen adsorbed on 50-nm PS particles, or a combination of the two.

The monotherapy with antigen adsorbed on 50-nm PS particles significantly outperformed therapy with anti-PD-1 monoclonal antibody by reducing MC38-OVA and B16F10-OVA tumor growth over time. The combination of both therapies did not add a therapeutic benefit against the MC38-OVA tumor compared to vaccination with OVA adsorbed on 50-nm PS particles. This is most likely due to the highly immunogenic nature of this hot tumor, which is clearly represented by the high probability of survival (> 66%) achieved in both groups of mice treated with standalone therapies. However, in the case of the B16F10-OVA tumor model, the combination of vaccination with OVA adsorbed on 50-nm PS particles and anti-PD-1 monoclonal antibody significantly decreased tumor growth and increased the probability of survival (17.5 days on average) compared with the mice receiving either of the monotherapies (anti-PD-1: 11.3 days; 50-nm PS with adsorbed OVA: 12.3 days). It is important to note that around day 15 of the study, the tumor growth in this group accelerates. This timing coincides with the final dose of anti-PD-1 treatment, suggesting that the immunosuppressive tumor microenvironment may have been reestablished, potentially leading to exhaustion of the vaccine-induced antigen-specific T cells. While this study did not explore extended treatment regimens, it is possible that more prolonged administration of both the cancer vaccine (e.g. weekly throughout the study) and the anti-PD-1 antibody (e.g. every 5 days) might be necessary to achieve sustained tumor control. This approach aligns with clinical strategies where cancer vaccines and immune checkpoint inhibitors are administered repeatedly over extended periods—sometimes continuing until disease progression—to maintain ongoing immune stimulation. For example, PROSTVAC (prostate-specific antigen [PSA]-TRICOM), a recombinant viral vector–based therapeutic vaccine for metastatic castration-resistant

prostate cancer (mCRPC), is administered subcutaneously starting with a priming dose, followed by multiple booster doses every 4 weeks for 6 months or longer, with the goal of sustaining and amplifying antigen-specific T-cell responses over time.[59,60]

The synergistic effect observed in the B16F10-OVA model highlights the importance of combining multiple treatments to treat cancer, especially cold tumors, to not only recruit cytotoxic T cells but also reverse the immunosuppressive microenvironment, keeping lymphocytes active for longer. An example of this is the enhanced antitumor response observed in mice vaccinated with an adenovirus-based vaccine targeting HPV-E6/E7 proteins in combination with anti-PD-1[61]; or the clinical evidence of successfully combining Pembrolizumab (anti-PD-1 monoclonal antibody) with T-VEC (Talimogene laherparepvec)- a genetically modified vaccine containing Herpes simplex virus Type 1 (HSV-1)-derived oncolytic viral proteins in which viral genes are partially deleted and replaced by the GM-CSF gene,[62] evaluated as a phase Ib trial for the treatment of stage IIIB to IV unresectable melanoma (62% of response rate compared to the 26% with T-VEC and 34% with Pembrolizumab used as monotherapies).[41,63]

It is important to highlight that the dose of 50-nm PS particles administered to the mice throughout these studies was low—200 μg per mouse in the prophylactic studies and 400 μg per mouse in the immunotherapeutic studies, but nevertheless, these were enough to significantly enhance cytotoxic CD8$^+$ T-cell activity, showing a strong effect therapeutically in a cancer setting when the antigen was adsorbed on the nanoparticle surface. This highlights the importance of optimizing adjuvant physicochemical properties in the design of particulate systems for production processes amenable to scalability and real-world practicality.

In this study, we used PS-based nanoparticles to demonstrate the benefits of adsorbing antigen to the nanoparticle surface, thereby enhancing the potency of nanoparticle-based cancer vaccines. PS is a cost-effective, stable material that allows for consistent particle size and is widely used as a model for polymeric nanoparticles. However, its nonbiodegradable nature makes it unlikely to receive clinical approval due to potential concerns over accumulation and long-term toxicity.[64] In contrast, biodegradable polymers such as PLGA offer a more clinically relevant alternative. Munoz-Wolf *et al.*[30] reported that i.m. vaccination with 50-nm PS particles elicited CD8$^+$ T-cell responses comparable to those induced by 50-nm PLGA particles. To translate our findings to biodegradable platforms, antigens could be adsorbed on PLGA nanoparticles using charged surfactants to promote electrostatic interactions, and formulation stability could be improved with optimized buffer conditions.

In conclusion, our findings demonstrate the importance of the rational design of polymeric particulate vaccine adjuvants—particularly through antigen adsorption to the nanoparticle surface—in enhancing antigen-specific CD8$^+$ T-cell responses and promoting antitumor immunity, with direct applications in the development of more effective therapeutic cancer vaccines.

METHODS

Mice

Eight- to 12-week-old female wild-type (WT), C57BL/6-Tg (TcraTcrb)1100Mjb/J (OT-I mice) and B6.129S(C)-Batf3tm1Kmm/J (Batf3$^{-/-}$) mice on a C57BL/6J background were provided by The Jackson Laboratory (Bar Harbor, ME, USA) and were bred in-house by the Comparative Medicine Unit (CMU) and maintained according to the regulations of the European Union and the Health Products Regulatory Authority (HPRA). They were kept in individual ventilated cages (IVC), specific-pathogen-free (SPF) conditions with a 12 h light cycle, 21°C, and unrestricted food and water consumption. All procedures were conducted under HPRA animal licenses number AE19136/P079 and AE19136/P172—approved by TCD Animal Research Ethics Committee (Ethical Approval Number 091210).

To generate B6.129S(C)-Batf3tm1Kmm/J (Batf3$^{-/-}$) mice, a targeting vector was designed to replace exons 1–2 of the basic leucine zipper transcription factor, ATF-like 3 (Batf3) gene with a loxP-flanked neomycin resistance (neo) cassette. The construct was electroporated into 129S6/SvEvTac-derived MC50 embryonic stem (ES) cells. Correctly targeted ES cells were injected into blastocysts, and the resulting chimeric males were bred to 129SvEv females to establish a colony. These mice were subsequently bred to BALB/c-Tg(CMV-cre)1Cgn/J mice (Stock No. 003465) to remove the neo cassette. These mice were backcrossed to C57BL/6 mice for at least 10 generations. Upon arrival at The Jackson Laboratory, mice were bred to C57BL/6J inbred mice (Stock No. 000664) for at least one generation to establish the colony.

Cell culture conditions

Cells were cultured in a steri-cycle CO_2 incubator HEPA class 100 (Thermo Fisher Scientific, Waltham, MA, USA) with 5% CO_2, 95% humidity, 37°C and darkness. Base medium used for cell culture —RPMI-1640 GlutaMAX (Gibco (Thermo Fisher Scientific), Waltham, MA, USA) or DMEM (Sigma-Aldrich (Merck KGaA), Darmstadt, Germany), was supplemented with 10% of filter-sterilized fetal bovine serum (FBS) or fetal calf serum (FCS) (Biosera, Cholet, France), 1% of Penicillin/Streptomycin (50 U mL^{-1} penicillin and 50 μg mL^{-1}streptomycin) (Gibco (Thermo Fisher Scientific),

Waltham, MA, USA) and 0.1% of β-mercaptoethanol (45.5 μM) (Gibco (Thermo Fisher Scientific), Waltham, MA, USA) to make complete media (cRPMI) and also with 1% (2 mM) glutamine (Gibco (Thermo Fisher Scientific), Waltham, MA, USA) to make cDMEM. T cell media was made by supplementing cRPMI with 1% Sodium Pyruvate (0.88 mM) (Thermo Fisher Scientific, Waltham, MA, USA), 1% nonessential amino acids (10 mM) (Thermo Fisher Scientific, Waltham, MA, USA) and 0.4% (v/v) of 100X MEM-Vitamins (Gibco (Thermo Fisher Scientific), Waltham, MA, USA).

MC38-OVA and B16F10-OVA tumor cell lines

MC38 and B16F10 cell lines derived from C57BL/6 murine colon adenocarcinoma and melanoma cells, respectively. MC38-OVA[65] and B16F10-OVA[66] cell lines were generated by transducing MC38 and B16F10 cells with lentivirus encoding chicken OVA protein.

MC38-OVA and B16F10-OVA cell lines were cultured in cDMEM and used for experiments *in vivo* upon reaching logarithmic growth between 50% and 70% confluency.

CHO-Flt3L cell line

Flt3L (Fms-related tyrosine kinase 3 ligand) was required for the culture of CD103$^+$ DCs (inducible cDC1s). This cytokine was obtained from a CHO (Chinese Hamster Ovarian) cell line that had been transfected with the murine gene for Flt3L (generated by Professor Nicos Nicola, WEHI, Australia).

Cells were seeded into two T25 flasks (Greiner Bio-One, Kremsmünster, Austria) containing RPMI-1640 GlutaMAX (Gibco (Thermo Fisher Scientific), Waltham, MA, USA) with 8% filter-sterilized FCS (Biosera, Cholet, France) and incubated at 37°C with 5% CO_2. After reaching 75% confluence, cells from each T25 flask were passaged (1:3) into a T75 flask. After 48 h, one T75 flask was used to freeze new stock vials of CHO-Flt3L cells, while the other was passaged (1:4) into two fresh T75 flasks containing RPMI with 4% FCS. When cells reached full confluence, each T75 flask was passaged (1:4) into two T75 flasks containing RPMI with 2% FCS. Next, fully confluent T75 flasks were each passaged (1:3) into three T175 flasks containing RPMI with 2% FCS, yielding 12 T175 flasks. Cells were incubated for 7 days, until culture medium turned pale orange but remained translucent. T175 flask supernatants were removed, transferred to 50 mL tubes and centrifuged at 125 *g* for 10 min to pellet carryover cells. Flt3L-containing supernatants were filter-sterilized using a stericup (MilliporeSigma (Merck KGaA), Burlington, MA, USA). The concentration of Flt3L was determined by ELISA (FLT3L DuoSet ELISA kit (R&D Systems (Bio-Techne Corporation), Minneapolis, MN, USA)) as per manufacturer's instructions, and supernatants were stored at −20°C until further use.

For each of the passages, flask supernatants were removed and cells were incubated with Trypsin-EDTA (Gibco (Thermo Fisher Scientific), Waltham, MA, USA) at 37°C until cells were detached. Trypsin-EDTA was quenched with RPMI and detached cells were centrifuged (125 *g*, 10 min) and resuspended in fresh RPMI before culturing in new flasks.

Vaccine formulation

1. Antigen

Apyrogenic ovalbumin (OVA) was obtained from Hyglos GmbH (Germany).

2. Polymeric nanoparticles

a. Particle washing

Ultrapure endotoxin-free, negatively charged polystyrene (PS) particles were purchased from Phosphorex Inc. (Hopkinton, MA, USA). The nanoparticle suspension (100 mg mL^{-1}) was transferred to 5-mL ultracentrifuge tubes and washed in 2 mL of PBS using two cycles of ultracentrifugation (234 000 *g* for 45 min at 15°C) to remove surfactants or stabilizers—the centrifugation velocity was determined as per Stoke's Law according to particle size.[67] Nanoparticles were resuspended in the appropriate volume of sterile PBS to achieve the desired polymer mass (25 mg mL^{-1}). Finally, particle suspensions were stored at 4°C.

b. Preparation of vaccine formulations

i. Formulation with soluble OVA

Fifty-nanometer PS particles were mixed with OVA in PBS (pH 7.4) to reach a 1:40 (antigen:nanoparticle) ratio—specific working concentrations can be found in the methods for each experiment below. Then, the mixture was vortexed for 30 s and left at room temperature (RT) for 15–30 min before adding to the cells or used for vaccination of mice.

ii. Formulation with adsorbed OVA

Fifty-nanometer PS particles were mixed with OVA in HEPES 125 mM buffer (pH 4.5–5.0) to reach a 1:40 (antigen:nanoparticle) ratio; specific working concentrations can be found in each of the experiment's methods below. Then, the mixture was vortexed for 30 s and left at RT for 5–8 h before adding to the cells or used for vaccination of mice.

Nanoparticle characterization

Samples of 50-nm PS particles (Phosphorex Inc., Hopkinton, MA, USA) (400 μg mL^{-1}) in either 1 mL of PBS (pH 7.4) or HEPES (125 mM, pH 4.5–5.0), as well as of the nanoparticles combined with OVA (Hyglos GmbH, Bernried am Starnberger See, Germany) (10 μg mL^{-1}) in 1 mL of PBS pH 7.4 incubated at RT for 15–30 min ("50-nm PS with soluble OVA") or HEPES pH 4.5–5.0 incubated at RT for 5–8 h ("50-nm PS with adsorbed OVA"), were prepared and placed in cuvettes to characterize nanoparticle size (nm),

Table 1. Panel for the quantification and characterization of activated OVA-specific CD8$^+$ T cells.

Target	Fluorochrome	Clone	Supplier	Volume per sample
F4/80 + B220	AF700	cl:A3-1 / RA3-6B2	Bio-Rad Laboratories, Hercules, CA, USA	1 µL
CD11c	BV605	N418	BioLegend, San Diego, CA, USA	1 µL
CD3	BV650	17A2	BioLegend, San Diego, CA, USA	1 µL
CD4	APC-eFluor780	GK1.5	eBioscience, San Diego, CA, USA	1 µL
CD8	PE-AF750	KT15	Bio-Rad Laboratories, Hercules, CA, USA	5 µL
CD44	FITC	IM7	BD Biosciences, Woburn, MA, USA	1 µL
SIINFEKL-specific CD8$^+$ T cells (TCR)	PE	H-2k^b tetramer	MBL International Corporation, Woburn, MA, USA	8 µL (1:12.5)
Live/Dead	BV510	N/A	BD Biosciences, Woburn, MA, USA	2 µL (1:500 dilution)

polydispersity index (PDI) and zeta potential (ZP) using a Zetasizer Nano ZS (Malvern Panalytical Ltd, Malvern, Worcestershire, UK) (Supplementary table 1).

Quantification of OVA adsorbed on 50-nm PS particles

Formulation of OVA (10 µg mL^{-1}) with 50-nm PS particles (400 µg mL^{-1}) (ratio 1:40, respectively) was prepared in a volume of 500 µL in 1.5-mL sterile microcentrifuge tubes under different conditions—either in HEPES, pH 4.5–5.0 or PBS, pH 7.4 at RT. After incubation for 2 and 8 h, formulations were added into 5-mL ultracentrifuge tubes and spun down by ultracentrifugation at 234 000 *g* for 45 min at 15°C. Supernatants were collected, and a Bicinchoninic acid (BCA) assay was performed to measure the concentration of soluble OVA present in the samples (following manufacturer's instructions—Pierce™ BCA Protein Assay Kit, Thermo Fisher Scientific, Waltham, MA, USA). Plates were then cooled down at RT and optical density (OD) values were obtained using a Multiskan FC plate reader (Thermo Fisher Scientific, Waltham, MA, USA) using Skanit Software 1.5.1, measuring absorbance at 562 nm wavelength. Soluble OVA concentrations were determined by comparing OD values with the BSA standard curve (5–250 µg mL^{-1}) allowing calculation of the percentage of OVA adsorbed on the 50-nm PS particles in both samples (Supplementary figure 1).

Assessment of T-cell responses *in vivo*

1. Prophylactic vaccination study

Intramuscular (i.m.) vaccination was performed on days 0 and 14 using 27G/0.5 in tuberculin syringes (Becton, Dickinson and Company, Franklin Lakes, NJ, USA) in both hind limbs (quadriceps femoris muscles) by injecting 50 µL per leg. Animals received either OVA alone (5 µg) or 50-nm PS particles (200 µg) with soluble or adsorbed OVA (5 µg).

2. Isolation of splenocytes

Spleens were collected from euthanized mice (using CO_2) 2 weeks after booster vaccination (day 28) and a single-cell suspension was obtained after homogenizing by mechanical dissociation with a sterile plunger and filtering the cell suspension in cRPMI through a 40-µm cell strainer (Thermo Fisher Scientific, Waltham, MA, USA). Cells were centrifuged, supernatants decanted, and cell pellets resuspended in 1 mL of 0.88% ammonium chloride (NH_4Cl) for 2 min to lyse erythrocytes, with subsequent quenching of the reaction by cRPMI and centrifugation. Cell pellets were resuspended in a 5 mL of T-cell medium, and live cells were counted by trypan blue exclusion. For *ex vivo* antigen restimulation assays, cells were plated in sterile round bottom 96-well plates in T-cell media at 10 × 10^6 cells mL^{-1} for intracellular staining studies. Cells were then restimulated with appropriate antigen concentrations, as detailed in the methods and figure legends for each experiment.

3. Quantification and characterization of antigen-specific CD8$^+$ T cells

Two weeks after booster vaccination, mice were euthanized using CO_2, spleens were collected, and splenocytes were isolated. 2 × 10^7 viable splenocytes were added to Flow Cytometry tubes with lids (Thermo Fisher Scientific, Waltham, MA, USA) in a T-cell medium to analyze antigen-specific CD8$^+$ T cells by tetramer staining. To do so, splenocytes were stained with PE-labeled H-2K^b Chicken OVA$_{257\text{-}264}$ SIINFEKL tetramers (MBL International Corporation, Woburn, MA, USA) at 1:12.5 dilution in a T-cell medium for 2 h in a cell culture incubator —5% CO_2, 95% humidity, darkness and 37°C, with orbital shaking (TITRAMAX 100—Heidolph Instruments) (250 rpm). During the last 40 min of the staining, anti-CD16/CD32 monoclonal antibodies (BD Biosciences, Woburn, MA, USA) were added to block FcγRII/III [1:100 in PBS + 2% FBS (FACS buffer)]. After 10 min of incubation, antibody staining of specific extracellular molecules was carried out to characterize different cellular populations and identify OVA-specific CD8$^+$ T cells (Table 1) with an incubation time of 30 min. Thereafter, cells were washed in PBS, and dead cells were stained with fixable viability stain BV510 (1:500 dilution in PBS) for 30 min. Cells were washed and fixed for 15 min at RT in 2% paraformaldehyde (PFA) (Thermo Fisher Scientific, Waltham, MA, USA). Finally, after a last wash in PBS, pellets were resuspended in 250 µL of FACS buffer. Samples were kept at 4°C until acquisition in a 4-laser/16laser/16-fluorescent parameter LSR-Fortessa analyzer until reaching 1 × 10^4 CD8$^+$

Table 2. Panel for the quantification and characterization of activated antigen-specific IFN-γ$^+$ CD8$^+$ T cells.

Target	Fluorochrome	Clone	Supplier	Volume per well
CD3e	FITC	145-2C11	BD Biosciences, San Diego, CA, USA	0.5 µL
CD4	APC-eFluor780	GK1.5	Thermo Fisher Scientific, Carlsbad, CA, USA	0.5 µL
CD8α	PerCP-Cy5.5	53–6.7	BioLegend, San Diego, CA, USA	0.5 µL
CD44	BV605	IM7	BD Biosciences, San Diego, CA, USA	0.5 µL
IFN-γ	PE	XMG1.2	BioLegend, San Diego, CA, USA	0.5 µL
Live/Dead	BV510	N/A	BD Biosciences, San Diego, CA, USA	0.025 µL (1:1000 dilution)

T cells. Analysis was carried out in FlowJo (V10X). The gating strategy followed to study antigen-specific CD8$^+$ T cells is shown in Supplementary figure 5a.

4. Quantification and characterization of antigen-specific IFN-γ$^+$ CD8$^+$ T cells

Following the same protocol as above, splenocytes from vaccinated mice were collected on day 28. Then, 1×10^6 splenocytes from each mouse were plated in a T-cell medium and in triplicate in sterile 96-well round bottom plates (Greiner Bio-One, Kremsmünster, Austria). Afterward, cells were stimulated for 2 h with cognate antigen OVA (200 µg mL^{-1}) and SIINFEKL peptide (1 µg mL^{-1}) followed by 12 h of treatment with the protein transport inhibitor GolgiPlug containing Brefeldin A (BD Biosciences, Woburn, MA, USA) (1 µg mL^{-1}). After this, splenocytes were washed in PBS + 1% FBS, and dead cells were stained with fixable viability stain BV510 (1:1000 dilution in PBS + 1% FBS) for 15 min on ice. Thereafter, cells were washed and incubated for 10 min with anti-CD16/CD32 monoclonal antibodies to block FcγRII/III (1:100 dilution) in PBS + 1% FBS. After this, antibody staining of specific extracellular molecules was performed to characterize T-cell populations and specifically investigate activated CD8$^+$ T cells (Table 2) with an incubation time of 15 min on ice. After being washed, cells were fixed and permeabilized using the eBioscience™ Foxp3/Transcription Factor Staining Buffer Set (Thermo Fisher Scientific, Carlsbad, CA, USA). Then, staining of intracellular IFN-γ was performed overnight at 4°C in permeabilization buffer to analyze the activated IFN-γ$^+$ T-cell populations in the samples (Table 2). Finally, cells were washed and transferred into flow cytometry tubes with a final volume of 250 µL of PBS + 1% FBS. Samples were kept at 4°C until acquisition in a 4 laser/16 fluorescent parameter LSR-Fortessa analyzer until reaching 1×10^4 CD8$^+$ T cells. Analysis was carried out in FlowJo (V10X). The gating strategy followed to study IFN-γ$^+$ T cells is shown in Supplementary figure 5b.

Dendritic cell-CD8$^+$ T cell co-culture

1. Bone marrow-derived CD103$^+$ DCs

The culture of CD103$^+$ DCs (inducible cDC1s) was performed following the protocol of Mayer *et al.*[68] Briefly, on day 0, the femurs and tibiae from culled mice were removed, cleaned, and the ends of the bones were cut to flush out the bone marrow (BM) into a sterile petri dish with a 10-mL syringe (Avantor, Inc., Radnor, PA, USA) containing cRPMI and attached to a 27G needle (BD (Becton, Dickinson and Company), Fraga, Spain). Then, BM aggregates were broken up by passing them through a 10-mL syringe attached to a 19G needle (BD (Becton, Dickinson and Company)) and suspended cells were transferred to a 50-mL tube. After a centrifugation step, erythrocytes were lysed in 0.88% ammonium chloride (NH_4Cl) for 2 min. cRPMI was added to stop the lysis reaction, and cells were centrifuged before being counted. 1×10^7 cells were seeded in sterile petri dishes (Sarstedt AG & Co. KG, Nümbrecht, Germany) in a final volume of 10 mL (1×10^6 cells mL^{-1}) of cRPMI supplemented with Flt3L (52.5 ng mL^{-1}), obtained from a CHO (Chinese Hamster Ovarian) cell line that had been transfected with the murine gene for Flt3L (see above), and Granulocyte-macrophage colony-stimulating factor (GM-CSF) (4 ng mL^{-1}). On days 5 and 7 of culture, cells were fed with 6 mL dish^{-1} of cRPMI. On day 9 of culture, cells were collected, counted and split into double the number of petri dishes at 0.4×10^6 cells mL^{-1} in a final volume of 10 mL of cRPMI supplemented with GM-CSF (4 ng mL^{-1}) and Flt3L (52.5 ng mL^{-1}). On day 13 of the culture, cells were fed with 2.5 mL of cRPMI/dish. Finally, on day 15 of culture, cells were taken from the dishes, counted and plated in 96-well round bottom plates (2×10^4 cells well^{-1}) in cRPMI supplemented with GM-CSF (4 ng mL^{-1}) and Flt3L (52.5 ng mL^{-1}). Cells were left in the incubator overnight before being stimulated on the following day.

2. Proliferation of OT-I CD8$^+$ T cells

On day 16 of culture, cells were incubated for 6 h with PBS as a negative control, OVA alone (10 µg mL^{-1}) or 50-nm PS particles (400 µg mL^{-1}) with either soluble or adsorbed OVA (10 µg mL^{-1}). At the time of adding the stimulations, cells were cultured in serum-free RPMI supplemented with GM-CSF (4 ng mL^{-1}) and Flt3L (52.5 ng mL^{-1}) to prevent serum proteins from displacing antigens from the nanoparticles via competitive desorption, and after 20 min, 10% FBS was added to each well (total volume of 125 µL well^{-1}).

Splenic CD8$^+$ T cells from OT-I mice were isolated in MACS buffer (0.5% BSA in PBS + 2 mM EDTA) using a CD8α$^+$ T cells isolation kit (Miltenyi Biotec B.V. & Co. KG, Bergisch Gladbach, Germany) by negative selection and following the manufacturer's protocol. Afterward, isolated

Table 3. Panel for the quantification and characterization of proliferating OT-I CD8$^+$ T cells.

Target	Fluorochrome	Clone	Supplier	Volume/concentration per sample
CD3e	PE	145-2C11	BD Biosciences, Woburn, MA, USA	0.7 μL
CD4	APC-eFluor780	GK1.5	Invitrogen (Thermo Fisher Scientific), Waltham, MA, USA	1 μL
CD8α	PE Cy5	53–6.7	eBioscience, San Diego, CA, USA	1.3 μL
Cell proliferation tracker	CFSE	N/A	eBioscience, San Diego, CA, USA	5 μM
Live/Dead	Zombie Yellow	N/A	BioLegend, San Diego, CA, USA	0.5 μL (1:500 dilution)

CD8$^+$ T cells were counted, and the desired number was stained with 5 μM of CFSE in PBS for 20 min at 37°C (water bath). Thereafter, a 30 mL of T-cell medium were added for 5 min at RT to absorb any unbound dye. Then, cells were centrifuged and pellets were resuspended in a T-cell medium at 1.6×10^6 cells mL^{-1}.

The plate with CD103$^+$ DCs was centrifuged at 400 *g* for 5 min, supernatants were discarded, and 125 μL well^{-1} of a T-cell medium was added. Then, 125 μL well^{-1} of CD8$^+$ T cell suspension (2×10^5 T cells) was added to achieve a final ratio of 1:10 (CD103$^+$ DCs:CD8$^+$ T cells)- as suggested by Höpken *et al.*,[69] in a total volume of 250 μL well^{-1}. The coculture was kept in the incubator for 72 h, cells were transferred from the wells to Flow Cytometry tubes to be further stained. Zombie yellow was used as a cell viability stain, and anti-CD3, CD4 and CD8 antibodies were used to characterize the CD8$^+$ T-cell population (Table 3). Finally, after a wash in PBS, pellets were resuspended in 250 μL of FACS buffer. Samples were kept at 4°C until acquisition in a 4 laser per16 fluorescent parameter LSR-Fortessa analyzer until reaching 1×10^4 CD8$^+$ T cells. Analysis was carried out in FlowJo (V10X). The gating strategy followed to study the proliferating CD8$^+$ T-cell population is shown in Supplementary figure 5c.

Assessment of the colocalization of OVA and 50-nm PS particles upon cellular uptake

In this study, 1×10^6 CD103$^+$ DCs (inducible cDC1s) were plated in cRPMI supplemented with GM-CSF (4 ng mL^{-1}) and Flt3L (52.5 ng mL^{-1}) in a sterile 24-well plate (Greiner Bio-One, Kremsmünster, Austria) and left in the incubator overnight. Afterward, the plate was centrifuged and the medium was replaced with serum-free RPMI supplemented with GM-CSF (4 ng mL^{-1}) and Flt3L (52.5 ng mL^{-1}) to prevent serum proteins from displacing antigens from the nanoparticles via competitive desorption. Then, the cells were stimulated for 20 min with 50-nm PS$_{FITC}$ [Phosphorex Inc., Hopkinton, MA, USA] (200 μg mL^{-1}) with either OVA$_{AF647}$ (OVA labeled with Alexa Fluor® 647 Protein Labeling Kit (Thermo Fisher Scientific, Waltham, MA, USA) following manufacturer's instructions) (5 μg mL^{-1}) in solution (prepared in PBS pH 7.4 for 15–30 min at RT) or adsorbed on the nanoparticle's surface (prepared in HEPES 125 mM pH 4.5–5.0 for 5–8 h at RT). Thereafter, the cells were transferred from the wells to Flow Cytometry tubes. After a wash with PBS, the cells were fixed in 2% PFA in PBS for 15 min at RT and in darkness. Finally, the cells were washed with PBS again and transferred into 1.5-mL microcentrifuge tubes (Thermo Fisher Scientific, Waltham, MA, USA) in a final volume of 50 μL of PBS. Acquisition in a 4 laser Amnis ImageStream cytometer was performed by using INSPIRE Software (Luminex Corporation, Austin, TX, USA). Analysis of the colocalization of OVA$_{AF647}$ and 50-nm PS$_{FITC}$ particles inside the cells was carried out using IDEAS Software (Luminex Corporation, Austin, TX, USA) following the gating strategy shown in Supplementary figure 4.

Therapeutic vaccine studies with MC38-OVA and B16F10-OVA cancer cells

In this study, 5×10^5 MC38-OVA or B16F10-OVA cancer cells in the exponential growth phase were administered by s.c. injection in the lateral flank of mice in a volume of 50 μL. Mice were monitored daily, and tumor growth was measured using a caliper, and volumes (mm^3) were recorded. When tumors reached 10–20 mm^3 (day 0) and 1 week after (day 7), mice received 10 μg OVA alone or in combination with 400 μg of 50-nm PS particles with either soluble or adsorbed OVA by i.m. vaccination. Mice were humanely euthanized (using CO_2) when the tumor reached 1500 mm^3 or if necrosis was noted. In this study, some mice received anti-PD-1 checkpoint inhibitor (Assay Genie Ltd, Dublin, Ireland) (200 μg) in a volume of 200 μL by i.p. injection on days 5, 10 and 15 after the first immunization. Tumor growth over time and survival rates were analyzed upon finalization of the study.

Statistical analysis

Statistical analysis was performed using GraphPad Prism software. Data are presented as either individual values with their mean and standard error of the mean (SEM) or the mean of each of the groups only. One-way ANOVA was used in the coculture experiments to compare the number of proliferating T cells between groups as well as in the prophylactic vaccination experiments to study activated antigen-specific CD8$^+$ T cells and IFN-γ$^+$ CD8$^+$ T cells. An unpaired two-tailed *t*-test was applied for the analysis of the fold increase of proliferating T cells in the co-culture assay. Two-way ANOVA was used in the therapeutic studies to demonstrate significant differences in tumor growth

over time between treatment groups. Tukey's correction for multiple comparisons was applied in these statistical tests. A simple survival analysis (Kaplan–Meier) with the log-rank (Mantel-Cox) test was used to determine significant differences in the probability of survival of treated mice between groups. Statistical significance was set at $P \leq 0.05$. *P*-values are represented as $^*P < 0.05$, $^{**}P < 0.005$, $^{***}P < 0.0005$ and $^{****}P < 0.0001$.

ACKNOWLEDGMENTS

We thank Dr Alan Hibbitts [Royal College of Surgeons in Ireland (RCSI)] for kindly providing access to the Zetasizer Nano ZS system and Dr Lorena Garcia-del Rio (Trinity College Dublin) for helping with the characterization of the nanoparticles. TS received support from the Deutsche Forschungsgemeinschaft (DFG, German Research Foundation) (Project ID: 318346496—SFB 1292, TP18); JH-C, RWW and ECL received support from Science Foundation Ireland through a Frontiers of the Future award (19/FFP/6484). RWW also received support from the Irish Research Council Government of Ireland Postgraduate Scholarship (GOIPG/2019/4236).

AUTHOR CONTRIBUTIONS

Jorge Huete-Carrasco: Methodology; investigation; writing – original draft; writing – review and editing; formal analysis. **Jingjing Zhu:** Investigation; methodology; writing – review and editing. **Benoit J Van den Eynde:** Investigation; methodology; writing – review and editing. **Christian Thomas Mayer:** Investigation; methodology; writing – review and editing. **Tim Sparwasser:** Investigation; methodology; writing – review and editing. **Ross W Ward:** Writing – review and editing; methodology. **Ed C Lavelle:** Conceptualization; funding acquisition; writing – review and editing; methodology; project administration; supervision; resources.

CONFLICT OF INTEREST

ECL is the inventor on patent application, WO2021123430, Polymeric nanoparticles as vaccine adjuvants. All other authors declare no competing interests.

DATA AVAILABILITY STATEMENT

The data that support the findings of this study are available from the corresponding author upon reasonable request.

REFERENCES

1. Rincon-Restrepo M, Mayer A, Hauert S, *et al.* Vaccine nanocarriers: coupling intracellular pathways and cellular biodistribution to control CD4 vs CD8$^+$ T cell responses. *Biomaterials* 2017; **132**: 48–58.
2. Pollard AJ, Bijker EM. A guide to vaccinology: from basic principles to new developments. *Nat Rev Immunol* 2020; **20**: 83–100.
3. Bonam SR, Partidos CD, Halmuthur SKM, Muller S. An overview of novel adjuvants designed for improving vaccine efficacy. *Trends Pharmacol Sci* 2017; **38**: 771–793.
4. Roth GA, Picece VCTM, Ou BS, Luo W, Pulendran B, Appel EA. Designing spatial and temporal control of vaccine responses. *Nat Rev Mater* 2021; **6**: 99–113.
5. Stano A, Scott EA, Dane KY, Swartz MA, Hubbell JA. Tunable T cell immunity towards a protein antigen using polymersomes vs solid-core nanoparticles. *Biomaterials* 2013; **34**: 4339–4346.
6. Huete-Carrasco J, Lynch RI, Ward RW, Lavelle EC. Rational design of polymer-based particulate vaccine adjuvants. *Eur J Immunol* 2023; **53**: e2350512.
7. FUTURE II Study Group. Quadrivalent vaccine against human papillomavirus to prevent high-grade cervical lesions. *N Engl J Med* 2007; **356**: 1915–1927.
8. Giannini SL, Hanon E, Moris P, *et al.* Enhanced humoral and memory B cellular immunity using HPV16/18 L1 VLP vaccine formulated with the MPL/aluminium salt combination (AS04) compared to aluminium salt only. *Vaccine* 2006; **24**: 340–348.
9. Garçon N, Van Mechelen M, Wettendorff M. Development and evaluation of AS04, a novel and improved adjuvant system containing MPL and aluminum salt. *Immunopotentiators Mod Vacc* 2006; **2006**: 235–255.
10. Garçon N, Di Pasquale A. From discovery to licensure, the adjuvant system story. *Hum Vaccin Immunother* 2017; **13**: 19–33.
11. Ko EJ, Kang SM. Immunology and efficacy of MF59-adjuvanted vaccines. *Hum Vaccin Immunother* 2018; **14**: 477–494.
12. Morel S, Didierlaurent A, Bourguignon P, *et al.* Adjuvant system AS03 containing α-tocopherol modulates innate immune response and leads to improved adaptive immunity. *Vaccine* 2011; **29**: 2461–2473.
13. Pifferi C, Fuentes R, Fernández-Tejada A. Natural and synthetic carbohydrate-based vaccine adjuvants and their mechanisms of action. *Nat Rev Chem* 2021; **5**: 197–216.
14. Leroux-Roels G, Clement F, Ofori-Anyinam O, *et al.* Evaluation of the immune response to RTS,S/AS01 and RTS,S/AS02 adjuvanted vaccines: randomized, double-blind study in malaria-naïve adults. *Hum Vaccin Immunother* 2014; **10**: 2211–2219.
15. Mettens P, Dubois PM, Demoitié MA, *et al.* Improved T cell responses to *Plasmodium falciparum* circumsporozoite protein in mice and monkeys induced by a novel formulation of RTS,S vaccine antigen. *Vaccine* 2008; **26**: 1517–1527.
16. Papi A, Ison MG, Langley JM, *et al.* Respiratory syncytial virus prefusion F protein vaccine in older adults. *N Engl J Med* 2023; **388**: 135–146.
17. Polack FP, Thomas SJ, Kitchin N, *et al.* Safety and efficacy of the BNT162b2 mRNA Covid-19 vaccine. *N Engl J Med* 2020; **383**: 2603–2615.
18. Baden LR, el Sahly HM, Essink B, *et al.* Efficacy and safety of the mRNA-1273 SARS-CoV-2 vaccine. *N Engl J Med* 2021; **384**: 403–416.

19. Heath PT, Galiza EP, Baxter DN, *et al.* Safety and efficacy of NVX-CoV2373 Covid-19 vaccine. *N Engl J Med* 2021; **385**: 117–127.
20. Datoo MS, Natama MH, Somé A, *et al.* Efficacy of a low-dose candidate malaria vaccine, R21 in adjuvant matrix-M, with seasonal administration to children in Burkina Faso: a randomised controlled trial. *Lancet* 2021; **397**: 1809–1818.
21. Vikkurthi R, Balaji S, Upadhyay A, *et al.* Inactivated whole-virion vaccine BBV152/Covaxin elicits robust cellular immune memory to SARS-CoV-2 and variants of concern. *Nat Microbiol* 2022; **7**: 1433–1445.
22. Dotiwala F, Upadhyay AK. A comprehensive review of BBV152 vaccine development, effectiveness, safety, challenges, and prospects. *Front Immunol* 2022; **13**: e940715.
23. Halperin SA, Smith B, Coyle P, *et al.* A phase I study of the safety and immunogenicity of recombinant hepatitis B surface antigen co-administered with an immunostimulatory phosphorothioate oligonucleotide adjuvant. *Vaccine* 2003; **21**: 2060–2066.
24. Prabhakaran M, Ramachandran V, Mukherjee S, *et al.* Adjuvanted SARS-CoV-2 spike protein vaccination elicits long-lived plasma cells in nonhuman primates. *Sci Transl Med* 2024; **16**: eabq0707.
25. Hopkins RJ, Daczkowski NF, Karem KL, *et al.* Randomized, double-blind, placebo-controlled, safety and immunogenicity study of 4 formulations of anthrax vaccine adsorbed plus CPG 7909 (AV7909) in healthy adult volunteers. *Vaccine* 2013; **31**: 3058–3066.
26. Hopkins RJ, Karem KL, O'Donnell S, *et al.* Randomized, double-blind, active-controlled study evaluating the safety and immunogenicity of three vaccination schedules and two dose levels of AV7909 vaccine for anthrax post-exposure prophylaxis in healthy adults. *Vaccine* 2016; **34**: 4826–4834.
27. Nazeri S, Zakeri S, Mehrizi AA, Sardari S, Djadid ND. Measuring of IgG2c isotype instead of IgG2a in immunized C57BL/6 mice with *Plasmodium vivax* TRAP as a subunit vaccine candidate in order to correct interpretation of Th1 versus Th2 immune response. *Exp Parasitol* 2020; **216**: 107893.
28. Si Y, Yu L, Zhang Y, *et al.* Lung cDC1 and cDC2 dendritic cells priming naïve CD8+ T cells in situ prior to migration to draining lymph nodes. *Cell Rep* 2023; **42**: 112455.
29. Duong E, Jimenez-Duran G, Moron-Garcia JC, *et al.* Type I interferon activates MHC class I-dressed CD11b+ conventional dendritic cells to promote protective anti-tumor CD8+ T cell immunity. *Immunity* 2022; **55**: 290–304.
30. Munoz-Wolf N, Ward RW, Brunner SM, *et al.* Non-canonical inflammasome activation mediates the adjuvanticity of nanoparticles. *Cell Rep Med* 2022; **3**: 100779.
31. Wørzner K, Donnadieu E, Latz E, *et al.* Adsorption of protein antigen to the cationic liposome adjuvant CAF®01 is required for induction of Th1 and Th17 responses but not for antibody induction. *Eur J Pharm Biopharm* 2021; **165**: 174–183.
32. Aggarwal P, Hall JB, McLeland CB, Dobrovolskaia MA, McNeil SE. Nanoparticle interaction with plasma proteins as it relates to particle biodistribution, biocompatibility and therapeutic efficacy. *Adv Drug Deliv Rev* 2009; **61**: 428–437.
33. Gunawan C, Lim M, Marquis CP, Amal R. Nanoparticle-protein corona complexes govern the biological fates and functions of nanoparticles. *J Mater Chem B* 2014; **2**: 6551–6571.
34. Jhunjhunwala S, Hammer C, Delamarre L. Antigen presentation in cancer: insights into tumour immunogenicity and immune evasion. *Nat Rev Cancer* 2021; **21**: 298–312.
35. Böttcher JP, Reis e Sousa C. The role of type 1 conventional dendritic cells in cancer immunity. *Trends Cancer* 2018; **4**: 784–792.
36. Murphy TL, Grajales-Reyes GE, Wu X, Tussiwand R, Murphy KM. Transcriptional control of dendritic cell development. *Annu Rev Immunol* 2016; **34**: 93–119.
37. Gajewski TF, Schreiber H, Fu YX. Immune resistance orchestrated by the tumour microenvironment. *Immunol Rev* 2006; **213**: 131–145.
38. Leach DR, Krummel MF, Allison JP. Enhancement of antitumor immunity by CTLA-4 blockade. *Science* 1996; **271**: 1734–1736.
39. Iwai Y, Ishida M, Tanaka Y, *et al.* Involvement of PD-L1 on tumour cells in the escape from host immune system and tumour immunotherapy by PD-L1 blockade. *Proc Natl Acad Sci USA* 2002; **99**: 12293–12297.
40. Haslam A, Prasad V. Estimation of the percentage of US patients with cancer who are eligible for and respond to checkpoint inhibitor immunotherapy drugs. *JAMA Netw Open* 2019; **2**: e192535.
41. Kim CG, Sang YB, Lee JH, Chon HJ. Combining cancer vaccines with immunotherapy: establishing a new immunological approach. *Int J Mol Sci* 2021; **22**: 8035.
42. Theisen DJ, Murphy TL, Murphy KM. WDFY4 is required for cross-presentation in response to viral and tumour antigens. *Science* 2018; **362**: 694–699.
43. Simon J, Bonifaz LC, Molinaro R, *et al.* Achieving dendritic cell subset-specific targeting in vivo by site-directed conjugation of targeting antibodies to nanocarriers. *Nano Today* 2022; **43**: 101446.
44. Anselmo AC, Mitragotri S. Nanoparticles in the clinic: an update. *Bioeng Transl Med* 2019; **4**: e10143.
45. Lavelle EC, Ward RW. Mucosal vaccines—fortifying the frontiers. *Nat Rev Immunol* 2022; **22**: 236–250.
46. Wang J, Zhang M, Li Y, *et al.* STING licensing of type I dendritic cells potentiates antitumor immunity. bioRxiv 2024. https://doi.org/10.1101/2024.01.02.573934.
47. Kamath AT, Henri S, Battye F, *et al.* Synchronization of dendritic cell activation and antigen exposure is required for the induction of Th1/Th17 responses. *J Immunol* 2012; **188**: 482–492.
48. Bachmann MF, Jennings GT. Vaccine delivery: a matter of size, geometry, kinetics and molecular patterns. *Nat Rev Immunol* 2010; **10**: 787–796.

49. Nembrini C, Layre E, Gilleron M, *et al.* Nanoparticle conjugation of antigen enhances cytotoxic T-cell responses in pulmonary vaccination. *Proc Natl Acad Sci USA* 2011; **108**: 16401–16406.
50. Camus M, Tosolini M, Mlecnik B, *et al.* Coordination of intratumoral immune reaction and human colorectal cancer recurrence. *Cancer Res* 2009; **69**: 2685–2693.
51. Galon J, Bruni D. Approaches to treat immune hot, altered and cold tumours with combination immunotherapies. *Nat Rev Drug Discov* 2019; **18**: 197–218.
52. Sharma P, Allison JP. The future of immune checkpoint therapy. *Science* 2015; **348**: 56–61.
53. Chae YK, Arya A, Iams W, *et al.* Current landscape and future of dual anti-CTLA4 and PD-1/PD-L1 blockade immunotherapy in cancer; lessons learned from clinical trials with melanoma and non-small cell lung cancer (NSCLC). *J Immunother Cancer* 2018; **6**: 39.
54. Schizas D, Charalampakis N, Kole C, *et al.* Immunotherapy for pancreatic cancer: a 2020 update. *Cancer Treat Rev* 2020; **86**: 102016.
55. Beer TM, Kwon ED, Drake CG, *et al.* Randomized, double-blind, phase III trial of ipilimumab versus placebo in asymptomatic or minimally symptomatic patients with metastatic chemotherapy-naive castration-resistant prostate cancer. *J Clin Oncol* 2017; **35**: 40–47.
56. Wang L, Yu W, Zhu W, *et al.* Hot and cold tumours: immunological features and the therapeutic strategies. *MedComm* 2023; **4**: e343.
57. Wei SC, Duffy CR, Allison JP. Fundamental mechanisms of immune checkpoint blockade therapy. *Cancer Discov* 2018; **8**: 1069–1086.
58. Lian J, Yue Y, Yu W, Zhang Y. Immunosenescence: a key player in cancer development. *J Hematol Oncol* 2020; **13**: 151.
59. DiPaola RS, Plante M, Kaufman H, *et al.* A phase I trial of pox PSA vaccines (PROSTVAC®-VF) with B7-1, ICAM-1, and LFA-3 co-stimulatory molecules (TRICOM™) in patients with prostate cancer. *J Transl Med* 2006; **4**: 1.
60. Parsons JK *et al.* A randomized, double-blind, phase II trial of PSA-TRICOM (PROSTVAC) in patients with localized prostate cancer: the immunotherapy to prevent progression on active surveillance study. *Eur Urol Focus* 2018; **4**: 798–801.
61. Rice AE, Heaton NS, Moquin A, *et al.* An HPV-E6/E7 immunotherapy plus PD-1 checkpoint inhibition results in tumor regression and reduction in PD-L1 expression. *Cancer Gene Ther* 2015; **22**: 447–456.
62. Johnson DB, Puzanov I, Kelley MC. Talimogene laherparepvec (T-VEC) for the treatment of advanced melanoma. *Immunotherapy* 2015; **7**: 611–619.
63. Ribas A, Dummer R, Puzanov I, *et al.* Oncolytic virotherapy promotes intratumoral T cell infiltration and improves anti-PD-1 immunotherapy. *Cell* 2017; **170**: 1109–1119.
64. Kik K, Bukowska B, Sicińska P. Polystyrene nanoparticles: sources, occurrence in the environment, distribution in tissues, accumulation and toxicity to various organisms. *Environ Pollut* 2020; **262**: 114210.
65. Petit PF, Fontana F, Lee CM, *et al.* T cell–mediated targeted delivery of anti–PD-L1 nanobody overcomes poor antibody penetration and improves PD-L1 blocking at the tumour site. *Cancer Immunol Res* 2022; **10**: 623–635.
66. Zhu J, Kim S, Kerner Z, *et al.* Tumour immune rejection triggered by activation of α2-adrenergic receptors. *Nature* 2023; **618**: 126–132.
67. Bridges S, Robinson L. Centrifuges. In: Sethi R, ed. A Practical Handbook for Drilling Fluids Processing. Amsterdam: Elsevier; 2020:475–488.
68. Mayer CT, Ghorbani P, Heidkamp GF, *et al.* Selective and efficient generation of functional Batf3-dependent CD103$^+$ dendritic cells from mouse bone marrow. *Blood* 2014; **124**: 3081–3091.
69. Höpken UE, Schmid C, Hosse RJ, Förster R, Lipp M. The ratio between dendritic cells and T cells determines the outcome of their encounter: proliferation versus deletion. *Eur J Immunol* 2005; **35**: 2377–2385.

SUPPORTING INFORMATION

Additional supporting information may be found online in the Supporting Information section at the end of the article.